Title	Choroidal vasculature in bietti crystalline dystrophy with CYP4V2 mutations and in retinitis pigmentosa with EYS mutations
Author(s)	Hirashima, Takako; Miyata, Manabu; Ishihara, Kenji; Hasegawa, Tomoko; Sugahara, Masako; Ogino, Ken; Yoshikawa, Munemitsu; Hata, Masayuki; Kuroda, Yoshimasa; Muraoka, Yuki; Ooto, Sotaro; Yoshimura, Nagahisa
Citation	Investigative Ophthalmology and Visual Science (2017), 58(10): 3871-3878
Issue Date	2017-08
URL	http://hdl.handle.net/2433/227073
Right	© 2017 The Authors. This work is licensed under a Creative Commons Attribution 4.0 International License.
Type	Journal Article
Textversion	publisher

Choroidal Vasculature in Bietti Crystalline Dystrophy With *CYP4V2* Mutations and in Retinitis Pigmentosa With *EYS* Mutations

Takako Hirashima, Manabu Miyata, Kenji Ishihara, Tomoko Hasegawa, Masako Sugahara, Ken Ogino, Munemitsu Yoshikawa, Masayuki Hata, Yoshimasa Kuroda, Yuki Muraoka, Sotaro Ooto, and Nagahisa Yoshimura

Department of Ophthalmology and Visual Sciences, Kyoto University Graduate School of Medicine, Sakyo-ku, Kyoto, Japan

Correspondence: Manabu Miyata, Department of Ophthalmology and Visual Sciences, Kyoto University Graduate School of Medicine, Shogoin Kawahara-cho 54, Sakyo-ku, Kyoto 606-8507, Japan; miyatam@kuhp.kyoto-u.ac.jp.

Submitted: January 18, 2017
Accepted: July 4, 2017

Citation: Hirashima T, Miyata M, Ishihara K, et al. Choroidal vasculature in Bietti crystalline dystrophy with *CYP4V2* mutations and in retinitis pigmentosa with *EYS* mutations. *Invest Ophthalmol Vis Sci*. 2017;58:3871–3878. DOI:10.1167/iovs.17-21515

Purpose. We compare the choroidal vascular area between Bietti crystalline dystrophy (BCD) patients with *CYP4V2* mutations, retinitis pigmentosa (RP) patients with *EYS* mutations, and normal controls, and investigate the correlation between choroidal vascular area and associated parameters.

Methods. This prospective case-series study included consecutive nine eyes of nine BCD patients with *CYP4V2* mutations (BCD group), 16 eyes of 16 RP patients with *EYS* mutations (*EYS*-RP group), and 16 eyes of 16 normal volunteers matched for age and axial length (control group). Using swept-source optical coherence tomography, we obtained en face images of the choroidal vasculature at the midpoint of the choriocapillaris layer—Sattler's layer (inner choroid) and Haller's layer (outer choroid). After binarization, we compared the inner and outer choroidal vascular areas among the three groups and identified associated factors.

Results. The outer choroidal vascular area was 43.34 ± 5.76%, 53.73 ± 4.92%, and 52.80 ± 4.10% in the BCD, *EYS*-RP, and control groups, respectively. This value was significantly smaller in the BCD group than in the *EYS*-RP and control groups ($P < 0.001$ in both; no significant difference between the *EYS*-RP and control groups). In the BCD group, the outer choroidal vascular area was correlated strongly with the subfoveal inner choroidal thickness ($P = 0.001$, $r = 0.91$, respectively). The inner choroidal vasculature could not be identified in eight of nine eyes in the BCD group.

Conclusions. The outer choroidal vascular narrowing might progress with the inner choroidal thinning in BCD, and the inner choroidal vasculature might be extinguished in advanced-stage BCD. Our findings may help to clarify the etiology of BCD.

Keywords: choroidal vasculature, Bietti crystalline dystrophy, retinitis pigmentosa, *CYP4V2*, *EYS*

Bietti crystalline dystrophy (BCD) is a rare retinal dystrophy characterized by the presence of shiny yellow deposits on the cornea and posterior pole of the retina.[1] The symptoms of BCD, including night blindness and progressive constriction of the visual field, are similar to those of retinitis pigmentosa (RP). BCD is caused by mutations of *CYP4V2*.[2] On the other hand, more than 50 causative genes for nonsyndromic RP have been identified.[3] A major causative gene for RP is *EYS* in the Japanese, Spanish, British, Chinese, Israeli, and Palestinian populations.[4–7] The main sites of expression of *CYP4V2* in the eye are the RPE and choroid[8] whereas *EYS* is expressed mainly in the outer segments of the photoreceptors.[9–11] A previous study using enhanced depth imaging spectral domain optical coherence tomography (SD-OCT) showed choroidal thinning in a BCD patient.[12] Furthermore, another previous report using swept-source optical coherence tomography (SS-OCT) identified differences in the patterns of pathologic damage between BCD patients with *CYP4V2* mutations and RP patients with *EYS* mutations, that is, the choroidal damage was more severe in the former than in the latter group.[13] However, that study only estimated choroidal thickness and did not estimate the difference in the choroidal vasculature.

It is difficult to visualize the entire choroidal structure because of the low penetration and high backscattering at the level of the RPE of SD-OCT, which is used widely in clinical examination. SS-OCT, which has a longer wavelength than SD-OCT, allows a three-dimensional (3D) high-contrast image of the choroid to be obtained.[14] Further algorithms have been developed for SS-OCT that allowed en face imaging of the choroid.[15–17] Recently, Kuroda et al.[18] reported an objective increase in choroidal vascular area in eyes with central serous chorioretinopathy using en face images obtained with SS-OCT. Their methods enabled us to investigate the choroidal vascular area of BCD patients with *CYP4V2* mutations.

We compared objectively the choroidal vascular areas in BCD patients with *CYP4V2* mutations with RP patients with *EYS* mutations and normal controls using en face SS-OCT imaging and investigated the correlation between the choroidal vascular area and its associated parameters.

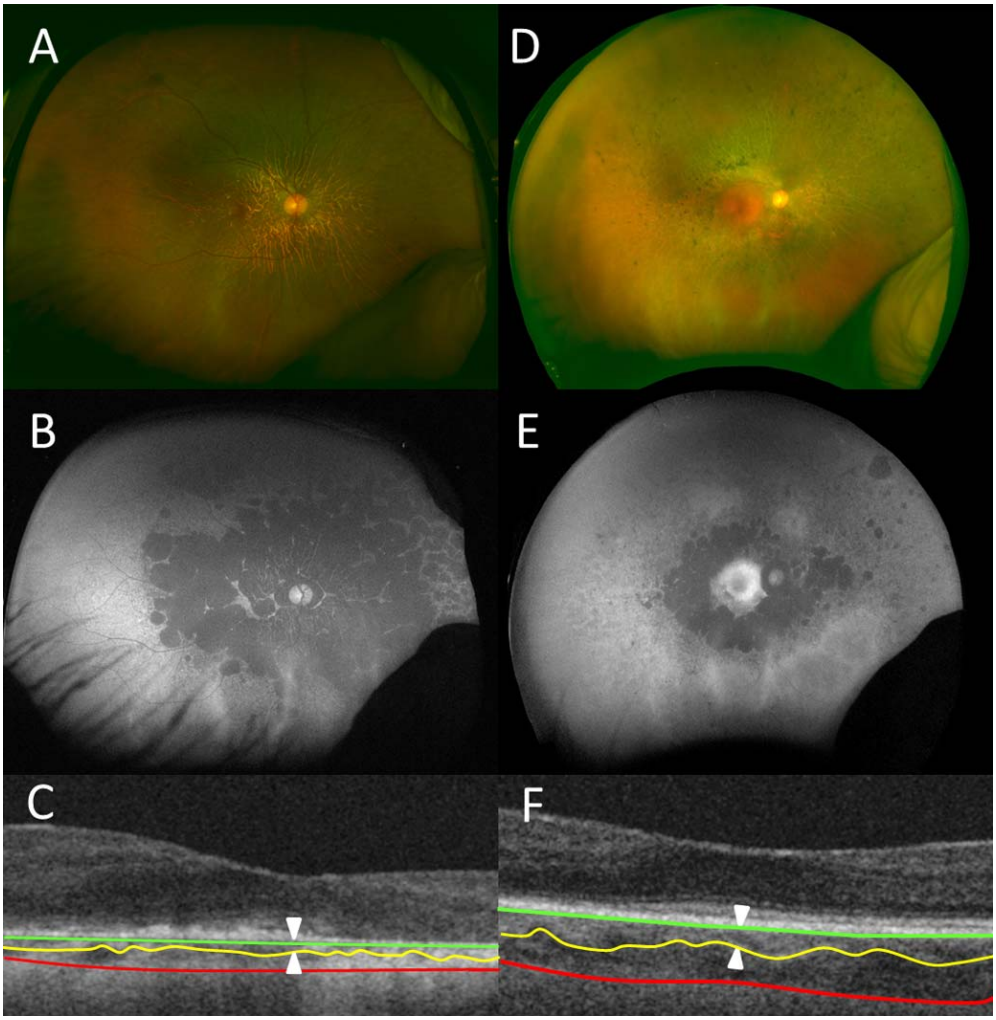

FIGURE 1. Representative images acquired by wide-field color fundus photography, wide-field fundus autofluorescence, and SS-OCT. (**A**) Color fundus photography image, (**B**) fundus autofluorescence image, and (**C**) SS-OCT image of the macula of the right eye in a 58-year-old woman with BCD with *CYP4V2* mutations with a VA of 20/13 and a MD value of −31.56 measured using a Humphrey field analyzer with the 10-2 Swedish Interactive Threshold Algorithm (SITA) standard program. (**D**) Color fundus photography image, (**E**) fundus autofluorescence image, and (**F**) SS-OCT image of macula of the right eye in a 71-year-old woman with RP with *EYS* mutations with a VA of 20/17 and a MD value of −18.43 measured using a Humphrey field analyzer with the 10-2 SITA standard program. (**C**, **F**) *Green lines* represent the outer border of the RPE/BM complex. *Yellow lines* represent the border between the medium and large choroidal vessel layers. *Red lines* represent the chorioscleral interface. The distance between the two *arrowheads* represents the subfoveal inner choroidal thickness. Two investigators manually measured the thickness with a high ICC.

METHODS

This prospective, observational case-series study was approved by the ethics committee at Kyoto University Graduate School of Medicine (Kyoto, Japan). All study protocols adhered to the tenets of the Declaration of Helsinki. The nature of the study and possible risks and benefits of participation were explained to all study candidates. All subjects who agreed to participate provided written informed consent.

Subjects

We recruited consecutive patients with degenerative retinal disease or retinal dystrophy who visited the Department of Ophthalmology and Visual Science at Kyoto University Graduate School of Medicine between September 2015 and October 2016. All patients provided blood samples for detection of gene mutations and underwent a comprehensive ophthalmologic examination, including autorefractometry; measurement of best-corrected visual acuity (VA) using a decimal VA chart (Landolt chart), and axial length (AL) using an IOL Master (Carl Zeiss Meditec, Inc., Dublin, CA, USA); indirect ophthalmoscopy; slit-lamp biomicroscopy; color fundus photography and fundus autofluorescence using an Optos device (Optos PLC, Dunfermine, UK, Fig. 1); SD-OCT (Spectralis HRA+OCT; Heidelberg Engineering, Heidelberg, Germany); and calculation of the mean deviation (MD) value with a Humphrey field analyzer (Carl Zeiss Meditec) using the 10-2 Swedish Interactive Threshold Algorithm standard program for the evaluation of macular sensitivity. Electroretinograms were recorded according to the International Society for Clinical Electrophysiology of Vision standard protocol recommended in 2008 using the LS-C (Mayo Co., Nagoya, Japan) and Neuropack MEB-2204 (Nihon Kohden, Tokyo, Japan) systems.[19] SS-OCT (DRI OCT-1; Topcon Corp., Tokyo, Japan; Fig. 1) also was performed. A clinical diagnosis of BCD or RP was made based on the above comprehensive ophthalmologic examinations by retinal specialists.

The inclusion criteria were as follows: BCD with homozygous or compound heterozygous mutations of *CYP4V2* or RP

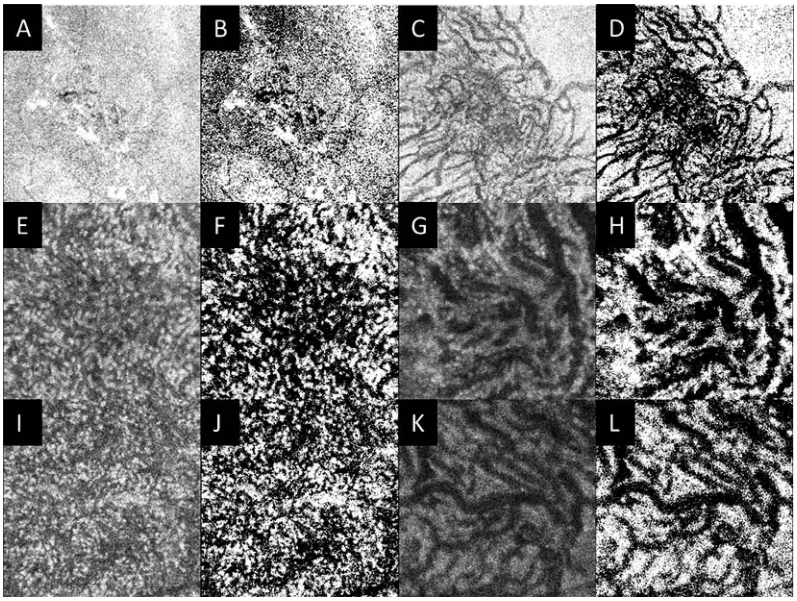

FIGURE 2. Representative choroidal en face images and binarized images at the level of the inner and outer choroid for measurement of choroidal vascular area. (**A**, **E**, **I**) Inner and (**C**, **G**, **K**) outer choroidal en face images of the right eye in a 58-year-old woman with BCD with *CYP4V2* mutations with a choroidal vascular area of "undetected" and 43.18% (**A**, **C**) before and (**B**, **D**) after binarization, respectively. Also, the right eye in a 47-year-old woman with RP with *EYS* mutations with a choroidal vascular area of 55.08% and 53.25% (**E**, **G**) before and (**F**, **H**) after binarization, and the right eye of a 77-year-old female control subject with a choroidal vascular area of 53.69% and 51.93% (**I**, **K**) before and (**J**, **L**) after binarization, respectively.

with homozygous or compound heterozygous mutations of *EYS*, and clear image quality on SS-OCT. The exclusion criteria were presence of other ocular diseases except for refractive errors, cataract, or pseudophakia, and AL $\geq$ 26.0 mm. When both eyes in one patient met the eligibility criteria, the right eye was selected for analysis. We also recruited healthy volunteers and patients with unilateral retinal disease, including epiretinal membrane and vitreomacular traction syndrome. We studied age-, sex-, and AL-matched healthy eyes (VA $\geq$ 20/20) for comparison with those of BCD or RP patients.

Images Obtained Using SS-OCT

Trained examiners performed the SS-OCT examinations after pupil dilation. They achieved pupil centration during the scan by using an internal fixation target that was confirmed using the camera built into the SS-OCT system. Each 3D volumetric scan covered an area of 3×3 mm^2 and was centered on the fovea. The 3D 3×3 mm^2 volumetric scans consisted of 512 (horizontal) $\times$ 256 (vertical) A-scans. In each B-scan of the 3D data set, the outer surface of the Bruch's membrane (BM) line was determined automatically by the software, and manual corrections were made as necessary using the built-in segmentation modifying tool. En face images were reconstructed automatically from the 3D data set using the software developed by Topcon Corporation.[18] En face images of the choroid were taken at varying depths every 2.6 μm from the BM, and were flattened at the level of the BM (Fig. 1). In Figure 2, the en face images show the vascular lumen as a black region and the vascular wall and choroidal stroma as a white region.

Measurement of Subfoveal Choroidal Thickness and Foveal Thicknesses

Horizontal B-scan images through the fovea obtained by SS-OCT were used to measure the subfoveal choroidal thickness and foveal thickness. Two investigators (T. Hirashima and M. Miyata) manually measured these thicknesses using the built-in caliper tool. The outermost highly reflective retinal band comprises the RPE and BM.[20] Foveal thickness was defined as the distance between the vitreoretinal interface and the outer border of the RPE/BM complex at the fovea. Subfoveal choroidal thickness was defined as the distance between the outer border of the RPE/BM complex and the chorioscleral interface at the subfovea. In addition, the same two investigators detected the border between the medium and large choroidal vessel layers as reported previously,[21,22] and manually measured the subfoveal distance between the outer border of the RPE/BM complex and the border between the medium and large choroidal vessel layers, using the several horizontal B-scans adjacent to the subfoveal scan as a reference. We defined this distance as the subfoveal inner choroidal thickness, which corresponds to the thickness of the choriocapillaris layer and the Sattler's layer (medium choroidal vessel layer; Fig. 1). For the subfoveal outer choroidal thickness, we subtracted the subfoveal inner choroidal thickness from the subfoveal total choroidal thickness. The subfoveal outer choroidal thickness corresponds to the Haller's layer (large choroidal vessel layer) thickness. The ratio of the subfoveal inner against the total choroidal thickness (%) was calculated. The mean measurements obtained by the two investigators were used for the analysis.

Measurement of Choroidal Vascular Area

To evaluate the area of the choroidal vasculature, we analyzed en face images at the level of the inner and outer choroid. Each en face image was created by extracting information from 3D raster scans at every 2.6-μm depth. We analyzed the choroidal vascular area from the en face images through the midpoints of the subfoveal inner and subfoveal outer choroid. The area of the choroidal vasculature in the adopted image was calculated automatically using ImageJ software (Wayne

Table 1. Characteristic of the Study Population

	BCD Group	*EYS*-RP Group	Control Group	*P* Value		
				BCD vs. *EYS*-RP	BCD vs. Control	*EYS*-RP vs. Control
n, eyes (subjects)	9 (9)	16 (16)	16 (16)			
Female sex, eyes (%)	6 (67)	10 (63)	12 (75)	0.98	0.91	0.74
Age, y	58.2 ± 4.6	52.4 ± 11.4	55.6 ± 14.2	0.46	0.85	0.72
AL, mm	23.96 ± 0.92	24.10 ± 1.23	24.09 ± 1.03	0.95	0.95	1.00
LogMAR VA	0.37 ± 0.57	0.34 ± 0.52	-	0.91		
MD value, dB	−28.06 ± 9.54	−16.80 ± 10.69	-	0.02†		
Lens status, phakic eyes	8	12	12	0.72	0.72	1.00
Foveal thickness, μm	125.4 ± 52.2	171.0 ± 44.1	195.8 ± 23.8	0.02*	<0.001*	0.19
Subfoveal choroidal thickness, μm						
Total	102.9 ± 2.6.7	208.5 ± 52.9	237.8 ± 61.8	<0.001*	<0.001*	0.27
Inner	23.4 ± 10.2	76.8 ± 23.5	80.6 ± 21.7	<0.001*	<0.001*	0.87
Outer	79.4 ± 22.4	131.7 ± 36.8	157.2 ± 49.0	<0.001*	0.009*	0.18
Ratio of the subfoveal inner against total choroidal thickness, %	22.8 ± 6.8	36.2 ± 8.9	34.4 ± 6.8	<0.001*	0.002*	0.78
Outer choroidal vascular area, %	43.34 ± 5.76	53.73 ± 4.92	52.80 ± 4.10	<0.001*	<0.001*	0.85

Data are presented as mean ± SD where applicable. BCD group, eyes of BCD patients with CYP4V2 mutations; EYS-RP group, eyes of RP patients with EYS mutations; Control group, healthy eyes; Inner choroid, from the outer border of the RPE and BM complex to the border between the medium and large vessel layers; Outer choroid, from the border between the medium and large vessel layers to the choriosclera interface.

* Statistically significant ($P < 0.05$, 1-way ANOVA).

† Statistically significant ($P < 0.05$, *t*-test).

Rasband, National Institutes of Health [NIH], Bethesda, MD, USA; available in the public domain at http://rsb.info.nih.gov/ij/index.html), according to a previous report.[18] Briefly, the command path of Image > Adjust > Threshold > Auto in ImageJ was used to distinguish the vasculature and choroidal stroma, and the adopted images were binarized using the Otsu method, which is an automatic threshold selection from gray-level histograms (Fig. 2).[23] Next, the area of the presumed vascular lumen portion was calculated in pixels using the command path of Analyze > Measure in ImageJ. In our study, the choroidal vascular area in the adopted images was defined as the portion of the vascular lumen area in the whole scan area in the inner and outer choroid, and is expressed as a percentage.

Statistical Analysis

Data are presented as means ± SD where applicable. VA was converted to logMAR for the statistical analyses. We performed 1-way ANOVA to compare the three groups. Corrections for multiple comparisons were made using a Tukey test. We used *t*-tests for comparison of two groups. Pearson's correlation coefficients were used for analysis of the association of inner and outer choroidal vascular area with other parameters, including age; AL; logMAR VA; MD value; foveal thickness; and subfoveal total, inner, and outer choroidal thicknesses. Spearman's rank correlation coefficients were used to analyze the association of inner and outer choroidal vascular area with sex (0, men; 1, women) and lens status (0, phakia; 1, pseudophakia). The intraclass correlation coefficients (ICC) for the measurements of the subfoveal choroidal thickness, foveal thickness, and subfoveal inner choroidal thickness were calculated to determine the interinvestigator reliability of the measurements. We calculated the cutoff value for the choroidal vascular area, the best sensitivity-specificity balance, and the area under the receiver-operating characteristic curve (AUROC). All statistical analyses were performed using the SPSS version 23 software (IBM Corp., Armonk, NY, USA). A *P* value of < 0.05 was considered to be statistically significant.

Results

The study included nine eyes of nine Japanese BCD patients with *CYP4V2* mutations (six women; BCD group), 16 eyes of 16 Japanese RP patients with *EYS* mutations (10 women; *EYS*-RP group), and 16 healthy eyes of 16 Japanese volunteers (12 women; control group). There were no blood relationships between any of the patients. The characteristics of the study population are shown in Table 1, and the clinical characteristics of the BCD and *EYS*-RP groups are shown in Table 2. The age of the subjects was 58.2 ± 4.6, 52.4 ± 11.4, and 55.6 ± 14.2 years in the BCD, *EYS*-RP, and control groups, respectively; 6 (67%), 10 (63%), and 12 (75%) eyes, respectively, were from female subjects; and the AL was 23.96 ± 0.92, 24.10 ± 1.23, and 24.09 ± 1.03 mm, respectively. There were no statistically significant differences in subject age, sex, or AL among the three groups. The logMAR VA in the BCD group was not significantly different from the *EYS*-RP group (0.37 ± 0.57 vs. 0.34 ± 0.52, $P = 0.91$). However, the MD value in the BCD group was significantly smaller than that in the *EYS*-RP group (−28.06 ± 9.54 vs. −16.80 ± 10.69 dB, $P = 0.02$).

Subfoveal Choroidal and Foveal Thicknesses

The subfoveal choroidal thickness was 102.9 ± 26.7, 208.5 ± 52.9, and 237.8 ± 61.8 μm in the BCD, *EYS*-RP, and control groups, respectively. The subfoveal choroidal thickness in the BCD group was significantly smaller than that in the *EYS*-RP ($P < 0.001$) and control ($P < 0.001$) groups, while there was no significant difference between the *EYS*-RP and control groups ($P = 0.27$). The subfoveal inner choroidal thickness was 23.4 ± 10.2, 76.8 ± 23.5, and 80.6 ± 21.7 μm in the BCD, *EYS*-RP, and

Table 2. Clinical Characteristics of BCD Patients With *CYP4V2* Mutations and RP Patients With *EYS* Mutations.

Case	Age, y	Sex	Eye	BCVA	AL, mm	HFA10-2 MD, dB	ERG, Cone Flicker Amplitude, μV	ERG, Cone Flicker Latency, ms	Mutation
BCD group									
1†	60	F	R	20/25	24.68	−33.52	18.2	28.8	c.802-8_810del17insGC / c.327+1G>A
2†	53	M	R	20/500	23.51	−34.33	7.4	34.0	c.802-8_810del17insGC / c.710C>A
3*	64	F	R	20/17	23.53	−4.22	96.0	25.6	c.802-8_810del17insGC / c.1226-6_1235del16
4*†	65	F	R	20/25	23.95	−26.81	67.5	30.2	c.802-8_810del17insGC / c.1226-6_1235del16
5*†	58	M	R	20/40	23.73	−24.4	39.8	28.0	c.802-8_810del17insGC / c.518T>G
6†	54	M	R	20/133	25.43	−32.26	25.7	28.4	c.802-8_810del17insGC homozygous
7*	60	F	R	20/13	22.94	−31.92	extinguished		c.802-8_810del17insGC homozygous
8†	52	F	R	20/200	25.08	−33.56	extinguished		c.802-8_810del17insGC homozygous
9*	58	F	R	20/13	22.77	−31.56	extinguished		c.802-8_810del17insGC homozygous
EYS-RP group									
1	43	F	R	20/17	24.77	−12.92	extinguished		c.4957dupA / c.1750G>T
2	69	M	R	20/100	23.04	−12.19	extinguished		c.4957dupA / c.8805C>A
3	71	F	R	20/17	24.11	−18.43	extinguished		c.4957dupA / c.8805C>A
4†	47	F	R	20/133	23.08	−31.22	extinguished		c.4957dupA / c.8805C>A
5†	51	M	R	20/22	23.97	−24.2	extinguished		c.4957dupA / c.8805C>A
6	66	M	R	20/25	24.07	−20.35	extinguished		c.4957dupA / c.8805C>A
7	31	F	R	20/13	25.56	−0.63	28.6	34.8	c.4957dupA / c.8805C>A
8	59	F	R	20/13	25.3	0.82	25.0	36.6	c.7793G>A / c.4957dupA
9	52	M	R	20/29	24.29	−24.62	extinguished		c.8805C>A / c.1345A>T
10	45	F	R	20/13	25.55	−0.78	11.0	28.8	c.8805C>A / c.4402_4403ins
11	41	F	L	20/40	25.69	−22.39	extinguished		c.4957dupA homozygous
12	47	F	R	20/50	21.8	−16.44	extinguished		c.7919G>A homozygous
13†	66	M	R	20/222	23.21	−31.77	extinguished		c.7919G>A homozygous
14	44	F	R	20/17	25.55	−4.93	25.0	27.4	c.8805C A homozygous
15†	58	M	L	20/400	23.1	−23.89	extinguished		c.8805C>A / c.5014C>T
16	49	F	R	20/333	22.46	−24.79	N.A.		c.4957dupA homozygous

BCD group, BCD with *CYP4V2* mutations group; BCVA, best-corrected VA; ERG, electroretinography; EYS-RP group, RP with *EYS* mutations group; F, female; HFA10-2, Humphrey field analyzer with the 10-2 SITA standard program; L, left eye; M, male; N.A., not available; R, right eye. There were no blood relationships among any of the patients.

* We performed other examinations in the same patients on a different date.[24]

† We performed other examinations in the same patients on a different date.[13]

control groups, respectively. The ratio of the subfoveal inner against total choroidal thickness in the BCD group was significantly smaller than that in the *EYS*-RP ($P < 0.001$) and control ($P = 0.002$) groups. Foveal thickness in the BCD group was significantly smaller than that in the *EYS*-RP ($P = 0.02$) and control ($P < 0.001$) groups. The ICC (2, 1) values for the subfoveal choroidal, foveal, and subfoveal inner choroidal thickness measurements were 0.981, 0.983, and 0.964, respectively.

Choroidal Vascular Area

The outer choroidal vascular area on en face images was analyzable in all subjects. The area was 43.34% ± 5.76%, 53.73% ± 4.92%, and 52.80% ± 4.10% in the BCD, *EYS*-RP, and control groups, respectively. The outer choroidal vascular area in the BCD group was significantly smaller than that in the *EYS*-RP ($P < 0.001$) and control ($P < 0.001$) groups, but was not significantly different between the *EYS*-RP and control ($P = 0.85$) groups. Table 3 shows the correlations between the outer choroidal vascular area and other parameters, respectively. In the BCD group, the outer choroidal vascular area was correlated strongly with the subfoveal inner choroidal thickness ($P = 0.001$, $r = 0.91$). The inner choroidal vasculature on en face images could not be identified in eight of nine eyes in the BCD group. Therefore, the statistical analysis in the BCD group did not include measurements of the inner choroidal vasculature. When the cutoff value for the outer choroidal vascular area was set at 46.67%, we could distinguish patients in the BCD group from those in the *EYS*-RP group with a specificity of 100% and a sensitivity of 77.8% (Fig. 3). From the AUROC curve, the best sensitivity–specificity balance achieved was 0.944.

Discussion

We found that the subfoveal choroidal thickness and the outer choroidal vascular area were smaller in BCD patients with *CYP4V2* mutations than in age-, sex-, AL-, and logMAR VA–matched RP patients with *EYS* mutations or age-, sex-, and AL-matched healthy controls. The difference in the degree of choroidal vascular damage between the BCD and *EYS*-RP patients could be accounted for by the difference in expression sites between *CYP4V2* and *EYS*.[8–11] Furthermore, among the studied parameters, the outer choroidal vascular area was correlated strongly with the inner choroidal thickness in BCD patients. This suggests that the outer choroidal vascular narrowing might progress with the inner choroidal atrophy in BCD. Furthermore, the inner choroidal vasculature could not be identified in most of the BCD patients. These findings may partly help to clarify the etiology of BCD.

The choroid is a highly vascular tissue located beneath the retina, and has an important role in providing the retina with nutrients. Although choroidal disorders do not directly affect visual function, long-term deficiencies in nutrient supply from

Table 3. Correlation Between Outer Choroidal Vascular Area and Other Parameters in BCD and *EYS*-RP Groups

	BCD Group, $n = 9$		*EYS*-RP Group, $n = 16$		Control Group, $n = 16$	
	P	***r***	***P***	***r***	***P***	***r***
Age	0.36	–	0.02*	0.57	0.80	–
Sex	0.64	–	0.68	–	0.023	−0.56
AL	0.18	–	0.85	–	0.76	–
LogMAR VA	0.35	–	0.73	–	–	–
MD value	0.14	–	0.42	–	–	–
Lens status	0.48	–	0.73	–	0.12	–
Foveal thickness	0.23	–	0.55	–	0.55	–
Subfoveal choroidal thickness						
Total	0.15	–	0.59	–	0.02*	0.57
Inner	0.001*	0.91	0.17	–	0.43	–
Outer	0.59	–	0.93	–	0.01	0.64

BCD group, eyes of BCD patients with *CYP4V2* mutations' *EYS*-RP group, eyes of RP patients with *EYS* mutations; Control group, healthy eyes; Inner choroid, from the outer border of the RPE and BM complex to the border between the medium and large vessel layers; Outer choroid, from the border between the medium and large vessel layers to the chorioscleral interface.

* Statistically significant ($P < 0.05$).

the choroidal vessels can lead to retinal damage. Our structural findings, an increased probability of the absence of the inner choroidal vasculature and increased outer choroidal vascular narrowing in BCD patients, suggested that the choroidal dysfunction of the outer retina may be more severe in BCD than *EYS*-RP patients. Furthermore, we reported previously that the photoreceptors in BCD patients with *CYP4V2* mutations were relatively preserved despite severe disease progression.[24] These results suggested that the retinal damage is delayed compared to the choroidal damage in BCD patients. Further research investigating blood flow dynamics in BCD patients is necessary.

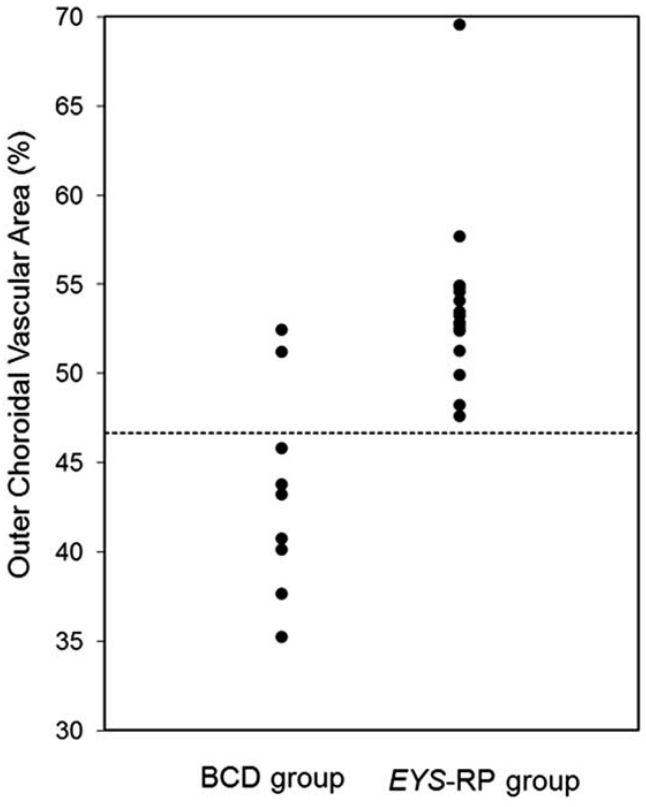

Figure 3. Cutoff values for the outer choroidal vascular area in the BCD and *EYS*-RP groups. When the cutoff value for the outer choroidal vascular area was set at 46.67%, we could distinguish between patients in the BCD and *EYS*-RP groups with a specificity of 100% and a sensitivity of 77.8%. From the AUROC curve, the best sensitivity–specificity balance achieved was 0.944.

Our study showed the significance of measuring the inner choroidal thickness, which to our knowledge has not been reported previously. Although the outer choroidal vascular area was not correlated with visual function including the VA and MD value, it was correlated strongly with the subfoveal inner choroidal thickness in BCD patients ($r = 0.91$). This implies that the inner choroidal thickness measured by B-scans could provide information on the state of the outer choroidal vasculature in BCD patients without having to estimate the vascular area. If the outer choroidal vascular area represents disease progression stage, the degree of the inner choroidal thinning could be used conveniently to classify the stage in BCD. Further research including various stages is necessary.

The ratio of the subfoveal inner against total choroidal thickness was significantly smaller in BCD than *EYS*-RP patients and healthy controls, which indicates that the degree of choroidal atrophy is higher in the inner choroid in BCD patients. To our knowledge, this finding has not been reported previously. Choroideremia has clinical features similar to those of BCD, and it can be difficult to distinguish the two diseases clinically. A previous report suggested that choroidal degeneration may be a secondary phenomenon in choroideremia, which lags significantly behind photoreceptor and RPE degeneration.[25] However, our previous study showed that the photoreceptors were relatively preserved in BCD patients.[24] The ratio that we determined may allow for differential diagnoses. Further research to compare the ratio between the two diseases is necessary.

Indocyanine green angiography is a standard modality for assessing choroidal vasculature, but cannot be used to assess individual layers. However, our study compared two different diseases with obviously different choroidal thickness.[13] Therefore, we adopted a method using en face images to analyze each layer of the choroidal vasculature separately. Furthermore, we modified the method of the previous study to analyze en face images through the midpoint of the total choroid[18]; that is, we first assessed the subfoveal inner choroidal thickness in each group, and then analyzed en face images through each midpoint of the inner and outer choroid. We believe that our method is suitable for analyzing the choroidal

vascular area, and in particular, to compare different diseases with different degrees of choroidal atrophy.

Our study has some limitations. The first limitation is that the sample size in the BCD group was small, reflecting the fact that BCD is a rare disease. However, it is unlikely that the inclusion of a larger sample size would have changed our results, given the marked difference between the BCD and *EYS*-RP groups. Second, we could not detect the inner choroidal vasculature in en face images in most of the BCD patients, either because the inner choroidal vasculature was too thin to be resolved on the images, or the vasculature of the choriocapillaris layer, Sattler's layer, was lost. A previous study using fluorescein angiography indicated the probability of choriocapillaris atrophy in advanced-stage BCD.[26] The development of modalities with high resolution and the corresponding analytical algorithms would allow us to clarify whether the inner choroidal vasculature is present in BCD patients. Third, there might be a difference of disease severity between the BCD and *EYS*-RP groups. Although age, sex, AL, and logMAR VA were matched, the MD value was different between the two groups. Further research with matched MD values is necessary.

In conclusion, the outer choroidal vascular area in BCD patients with *CYP4V2* mutations is smaller than that in RP patients with *EYS* mutations and in healthy controls, and the inner choroidal vasculature might be extinguished in advanced-stage BCD patients. Furthermore, the outer choroidal vascular narrowing might progress with the inner choroidal thinning in BCD. Our present findings may help to clarify the etiology of BCD.

Acknowledgments

The authors thank Akitaka Tsujikawa, Akio Oishi, and Maho Oishi for their helpful discussion regarding our methodology.

Supported in part by a grant-in-aid for scientific research (No. 26861451) from the Japan Society for the Promotion of Science, Tokyo, Japan, and the Innovative Techno-Hub for Integrated Medical Bio-Imaging of the Project for Developing Innovation Systems from the Ministry of Education, Culture, Sports, Science, and Technology (MEXT), Tokyo, Japan. None of these organizations had any role in the design or conduct of this research.

Disclosure: **T. Hirashima**, None; **M. Miyata**, None; **K. Ishihara**, None; **T. Hasegawa**, None; **M. Sugahara**, None; **K. Ogino**, None; **M. Yoshikawa**, None; **M. Hata**, None; **Y. Kuroda**, None; **Y. Muraoka**, None; **S. Ooto**, Alcon Japan (F); **N. Yoshimura**, Topcon Corporation (F), Nidek (F, C), Canon (F)

References

1. Bietti G. Ueber familiaeres vorkommen von "retinitis punctata albescens" (verbunden mit "dystrophia marginalis cristallinea corneae"), glitzern des glaskoerpers und anderen degenerativen augenveraenderungen [in German]. *Klin Monbl Augenheilkd*. 1937;99:737–753.
2. Li A, Jiao X, Munier FL, et al. Bietti crystalline corneoretinal dystrophy is caused by mutations in the novel gene CYP4V2. *Am J Hum Genet*. 2004;74:817–826.
3. Daiger SP, Sullivan LS, Bowne SJ. Genes and mutations causing retinitis pigmentosa. *Clin Genet*. 2013;84:132–141.
4. Oishi M, Oishi A, Gotoh N, et al. Comprehensive molecular diagnosis of a large cohort of Japanese retinitis pigmentosa and Usher syndrome patients by next-generation sequencing. *Invest Ophthalmol Vis Sci*. 2014;55:7369–7375.
5. Barragan I, Borrego S, Pieras JI, et al. Mutation spectrum of EYS in Spanish patients with autosomal recessive retinitis pigmentosa. *Hum Mutat*. 2010;31:1772–1800.
6. Abd El-Aziz MM, O'Driscoll CA, Kaye RS, et al. Identification of novel mutations in the ortholog of Drosophila eyes shut gene (EYS) causing autosomal recessive retinitis pigmentosa. *Invest Ophthalmol Vis Sci*. 2010;51:4266–4272.
7. Bandah-Rozenfeld D, Littink KW, Ben-Yosef T, et al. Novel null mutations in the EYS gene are a frequent cause of autosomal recessive retinitis pigmentosa in the Israeli population. *Invest Ophthalmol Vis Sci*. 2010;51:4387–4394.
8. Nakano M, Kelly EJ, Wiek C, Hanenberg H, Rettie AE. CYP4V2 in Bietti's crystalline dystrophy: ocular localization, metabolism of omega-3-polyunsaturated fatty acids, and functional deficit of the p.H331P variant. *Mol Pharmacol*. 2012;82:679–686.
9. Abd El-Aziz MM, Barragan I, O'Driscoll CA, et al. EYS, encoding an ortholog of Drosophila spacemaker, is mutated in autosomal recessive retinitis pigmentosa. *Nat Genet*. 2008; 40:1285–1287.
10. Yu M, Liu Y, Li J, et al. Eyes shut homolog is required for maintaining the ciliary pocket and survival of photoreceptors in zebrafish. *Biol Open*. 2016;5:1662–1673.
11. Alfano G, Kruczek PM, Shah AZ, et al. EYS Is a Protein associated with the ciliary axoneme in rods and cones. *PLoS One*. 2016;11:e0166397.
12. Zerbib J, Ores R, Querques G, Bouzitou-Mfoumou R, Souied EH. Choroidal findings in Bietti's crystalline dystrophy. *Retinal Case Brief Rep*. 2014;8:130–131.
13. Miyata M, Hata M, Ooto S, et al. Choroidal and retinal atrophy of Bietti crystalline dystrophy patients with CYP4V2 mutations compared to retinitis pigmentosa patients with EYS mutations. *Retina*. 2017;37:1193–1202.
14. Ueda-Arakawa N, Ooto S, Ellabban AA, et al. Macular choroidal thickness and volume of eyes with reticular pseudodrusen using swept-source optical coherence tomography. *Am J Ophthalmol*. 2014;157:994–1004.
15. Ferrara D, Mohler KJ, Waheed N, et al. En face enhanced-depth swept-source optical coherence tomography features of chronic central serous chorioretinopathy. *Ophthalmology*. 2014;121:719–726.
16. Choi W, Mohler KJ, Potsaid B, et al. Choriocapillaris and choroidal microvasculature imaging with ultrahigh speed OCT angiography. *PLoS One*. 2013;8:e81499.
17. Motaghiannezam R, Schwartz DM, Fraser SE. In vivo human choroidal vascular pattern visualization using high-speed swept-source optical coherence tomography at 1060 nm. *Invest Ophthalmol Vis Sci*. 2012;53:2337–2348.
18. Kuroda Y, Ooto S, Yamashiro K, et al. Increased choroidal vascularity in central serous chorioretinopathy quantified using swept-source optical coherence tomography. *Am J Ophthalmol*. 2016;169:199–207.
19. Marmor MF, Fulton AB, Holder GE, Miyake Y, Brigell M, Bach M. ISCEV Standard for full-field clinical electroretinography (2008 update). *Doc Ophthalmol*. 2009;118:69–77.
20. Drexler W, Sattmann H, Hermann B, et al. Enhanced visualization of macular pathology with the use of ultrahigh-resolution optical coherence tomography. *Arch Ophthalmol*. 2003;121:695–706.
21. Branchini LA, Adhi M, Regatieri CV, et al. Analysis of choroidal morphologic features and vasculature in healthy eyes using spectral-domain optical coherence tomography. *Ophthalmology*. 2013;120:1901–1908.
22. Esmaeelpour M, Kajic V, Zabihian B, et al. Choroidal Haller's and Sattler's layer thickness measurement using 3-dimensional 1060-nm optical coherence tomography. *PLoS One*. 2014;9: e99690.
23. Otsu N. A threshold selection method from gray-level histograms. *IEEE Trans Syst Man Cybern Syst Hum*. 1979; 9:62–66.

24. Miyata M, Ooto S, Ogino K, et al. Evaluation of photoreceptors in bietti crystalline dystrophy with CYP4V2 mutations using adaptive optics scanning laser ophthalmoscopy. *Am J Ophthalmol*. 2016;161:196–205.
25. Xue K, Oldani M, Jolly JK, et al. Correlation of optical coherence tomography and autofluorescence in the outer retina and choroid of patients with choroideremia. *Invest Ophthalmol Vis Sci*. 2016;57:3674–3684.
26. Wilson DJ, Weleber RG, Klein ML, Welch RB, Green WR. Bietti's crystalline dystrophy. A clinicopathologic correlative study. *Arch Ophthalmol*. 1989;107:213–221.

Investigative Ophthalmology & Visual Science